Strategies to Synthesize CoNi-Pt Core@Shell Stable Mesoporous Nanorods with very Highly Active Surface for Methanol Electro-oxidation

Albert Serrà, Elvira Gómez, Elisa Vallés[*]

Departament de Química Física and Institut de Nanociència i Nanotecnologia (IN^{2}UB), Universitat de Barcelona, Martí i Franquès 1, 08028, Barcelona, Spain.

Corresponding Author

e.valles@ub.edu

Abstract

Three strategies have been tested to obtain stable mesoporous CoNi@Pt nanorods with a very high effective area and good performance for methanol electro-oxidation. They are based on, firstly, an electrochemical synthesis of the CoNi nanorods using three clearly different systems (micellar solution, water-in-ionic liquid microemulsion and suspension of polystyrene nanoparticles), and, secondly, a posterior platinum shell formation by interfacial replacement reaction. The obtained nanorods have been compared with pure platinum ones prepared following the three methods. Mesoporous CoNi@Pt nanorods with a very high active surface have been obtained by using the suspension of polystyrene nanoparticles and especially the water-in-ionic liquid microemulsion.

All the mesoporous nanorods (of both Pt and CoNi@Pt) show very good performance for methanol oxidation in comparison with compact ones or the usual Pt/C catalyzers. However, the

mesoporous CoNi@Pt nanorods have demonstrated better performance than the corresponding platinum ones for methanol oxidation due to the more active platinum atoms in the shell of platinum than in the bulk, the higher good poison tolerance and the lower cost of the material - owing to the drastic saving in platinum in the nanostructures. The mesoporous CoNi@Pt nanorods obtained from the water-in-ionic liquid microemulsion are the best candidates as electrocatalysers because they provide a significantly higher mass-normalized current density (1326 mA mg^{-1}), a good stability in the sulfuric acidic medium and a significant electrocatalytic stability under continuous operating conditions.

Keywords: Core@shell nanorods, Mesoporous nanorods, Methanol electro-oxidation, Electrodeposition, Water-in-ionic liquid microemulsions

In the emerging field of nanomaterials synthesis, metallic nanostructures (nanoparticles,[1-3] nanorods,[4,5] nanofibers,[6,7] nanotubes,[8,9] amongst others), especially those composed of noble metals, have sparked a great deal of attention for their unique properties for modern technology, ranging from catalysis or energy conversion to biological labeling or information storage.

Continuous growth in global energy demands has attracted concerns about energy and environmental sustainability, remarkably in the development of innovative energy technologies. Large efforts are currently being made in the energy conversion field, particularly in the development of electrocatalysts for Direct Methanol Fuel Cells (DMFCs), based on the use of nanomaterials.[10-13] Direct methanol fuel cells have attracted great scientific interest due to their low operating temperature, low pollution emissions, high power density and easy handling, which provided potential applications in electronic vehicles, among other portable devices.[14-16] However, the high cost of electrocatalysts and the insufficient efficiency hindered the commercialization of its electrochemical energy conversion. Furthermore, the most efficient catalysts for both anode and cathode are by far platinum and platinum-based materials.[17,18] Nevertheless, the high cost and the limited natural abundance of platinum limits its widespread use in large-scale applications; therefore, there exists a considerable interest in developing new

effective electrocatalysts (enhancing electrocatalytic activity and durability and reducing the cost).[19,20] Recently, the development of platinum-based nanomaterials, with nonprecious metals or metal oxides (Ni, Fe, Co, Ni_2O_3, CoO, amongst others), platinum with high porosity grade (mesoporous, nanoporous) and different shapes in the nanometer range, or other alternatives based on the development of nonprecious metals or oxides as catalysts have been drawing larger interest.[21-23] The platinum-based nanomaterials, especially bimetallic alloys with less expensive 3d-transition metals, present an enhanced electrocatalytic activity for methanol oxidation reaction (MOR) as a consequence of the reduction of poisoning by adsorbed carbonaceous intermediates, and the consequent reduction in the cost of electrocatalysts.[24-27] However, the durability of this electrocatalysts, especially in acid media, could hinder their potential application. Furthermore, in general, platinum rich alloys with a high degree of alloying are mandatory in order to improve the durability.[28,29] On the other hand, the development of well-defined nano or mesoporous nanostructures of metals, a peculiarity of noble metals, is proposed to prepare electrocatalysts showing a superior electrocatalytic performance as a consequence of their large area per unit of volume and the reduction of the load of electrocatalysts in fuel cells, with the consequent reduction of the cost.[30-34] Lastly, the use of nonprecious metals or oxides supported in carbon have been proposed to reduce the cost without significantly lowering catalytic performance, particularly for an oxygen reduction reaction (ORR), compared to platinum-based electrocatalysts.[35-37]

Herein, inspired by these proposals, we report a facile fabrication procedure of different CoNi@Pt mesoporous electrocatalysts with a nanowire shape using different strategies. The combination of the use of core@shells structures (with non-noble metals and a nanometer shell of platinum) and the synthesis of highly porous nanomaterials (mesoporous or nanoporous) in a single pot could be a powerful strategy to accomplish an important reduction of the amount of platinum in an easy way with excellent catalytic performance. Recently, the use of core@shell structures has been reported as a promising alternative in order to obtain electrocatalysts for energy conversion due to their improved electrocatalytic activity.[38,39] Furthermore, the

core@shell structures permit a further decrease in the noble metal loading in the electrodes without significant decay in the performance. Moreover, synergetic effects have been demonstrated when the subsurface of platinum atoms have been substituted by 3d-transition atoms (in our proposal for a magnetic CoNi alloy). On the other hand, the traditional hard-templating methods or some recent strategies based on the use of lyotropic liquid crystals (with high viscosity) hinder a facile procedure to obtain nano or mesoporous nanorods by electrochemical methods.[40-43] Recently, some studies proposed the use of the assembly of surfactant micelles or microemulsions based on ionic liquids inside the confined space of commercial polycarbonate membranes in order to obtain mesoporous nanorods.[44-45] Therefore, our proposal demonstrates the viability of core@shell CoNi@Pt mesoporous nanorods with different morphologies compared with the same nanorods of platinum as electrocatalysts for methanol oxidation. Furthermore, the use of CoNi@Pt nanorods could significantly reduce the amount of platinum (with a nanometer layer of platinum) without significant changes in the catalytic performance and introduce an easy handling tool as a consequence of their magnetic behavior which favors the anchoring or recollecting by the use of an external magnetic field.[46,47]

RESULTS AND DISCUSSION

Herein, we report all-wet electrochemical approaches in attempting to synthesize high mesoporous nanorods, in the confined space of commercial polycarbonate membranes with a nominal pore size of 100 nm, by using 1) an assembly of micelles (W+ S) method, which in earlier works was demonstrated to be useful for preparing mesoporous Pt nanorods in restricted conditions,[45] 2) water-in-ionic liquid microemulsions (W/IL microemulsions),[46] and 3) polystyrene nanoparticle (PS NPs) suspensions (W+PS). A classical CoNi bath has been selected to prepare magnetic mesoporous CoNi@Pt core@shell nanorods in order to achieve better activity, stability and efficiency as electrocatalysts for methanol oxidation. An electrolyte solution containing only 20 mM of Na_2PtCl_6 was also used to prepare the same mesoporous nanostructures for each approach in order to compare the platinum nanostructures to the core@shells ones. Furthermore, the use of both solutions permits comparing the different

proposed approaches in a diluted media (20 mM of Na_2PtCl_6) or a classical electrochemical bath (concentrated). Lastly, compact nanorods (W NWs) with both solutions were also prepared as a reference. The fabrication procedure of the eight types of nanorods is schematically illustrated in **Figure 1**: The pure-platinum nanorods were synthesized by electrodeposition at -200 mV from the four selected systems of platinum salt (W, W+S, W/IL microemulsion and W+PS). The CoNi@Pt nanorods were synthesized in two stages: the electrodeposition, at -960 mV, of the CoNi nanorods from the four selected systems of Co(II) and Ni(II) salts, and after that, the immersion (for 90 s) of the nanorods in a platinum salt solution (1 mM of $Na_2PtCl_{6)}$ in order to form the shell of platinum.

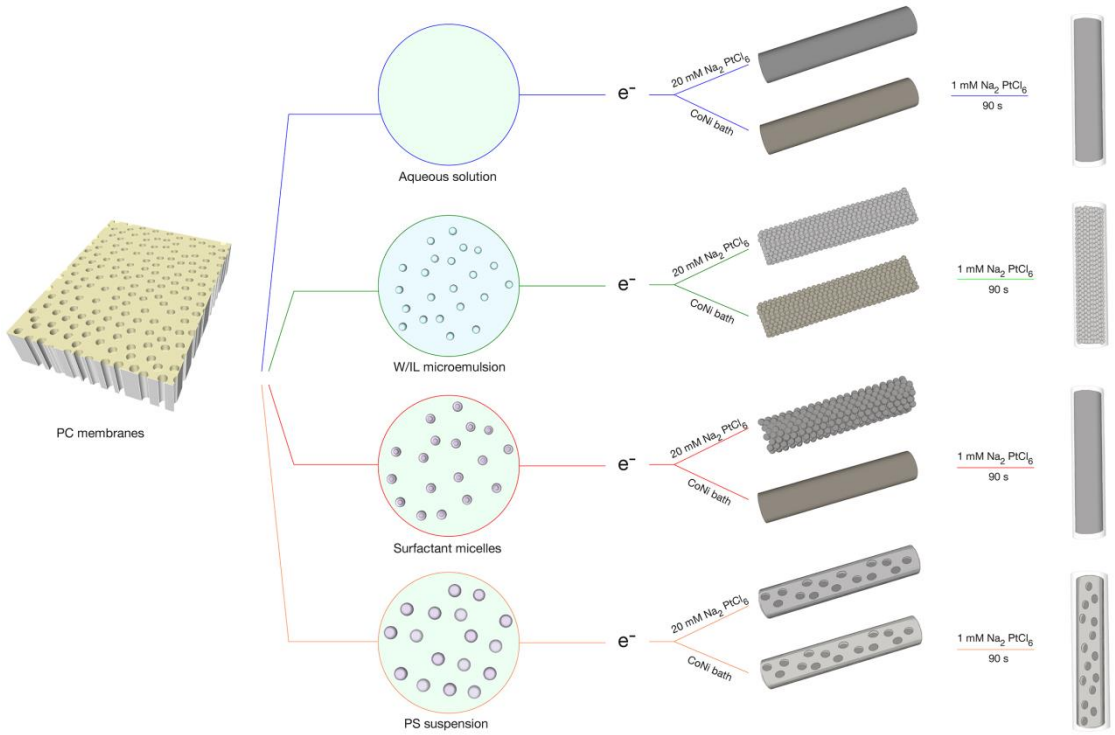

Figure 1: Schematic representation of the fabrication procedure of the eight types of nanorods.

Each electrodeposition process was performed at room temperature and in semi-stirring conditions (Ar bubbling), using the nanochannels of commercial polycarbonate membranes, until attaining a constant deposition charge density of 9 C cm^{-2}. As can be seen in the chronoamperometric curves (**Figure 1S**), the electrodeposition time until circulating the same deposition charge density is quite different depending on the selected system. The process is

significantly slower in the microemulsion system. Table 1 summarizes the composition of the nanorods obtained for the different selected electrodeposition media. In the case of the core@shell nanorods, the platinum percentage depends on their structure, which is a first indication of their different effective area, being the maximum value in the case of the W/IL nanorods.

TABLE 1. Selected electrodeposition media and nanorods composition

System		[W] / wt. %	[S] / wt. %	[IL] / wt. %	[PS NPs] / wt. %	Pt / at. %	Co / at. %	Ni / at. %
W	Pt	100	-	-	-	100	-	-
	CoNi@Pt	100	-	-	-	4	56	40
W/IL	Pt	27	61	12	-	100	-	-
	CoNi@Pt	27	61	12	-	8	55	37
W+S	Pt	99	1	-	-	100	-	-
	CoNi@Pt	99	1	-	-	3	56	41
W+PS	Pt	88	2	-	10	100	-	-
	CoNi@Pt	88	2	-	10	6	54	40

The morphology of the nanorods (Pt and CoNi@Pt) is characterized by using transmission electron microscopy (TEM) as shown in **Figure 2**. The lengths of the different nanorods ranged from 1.8 to 2.2 µm. The representative TEM images exhibit significant differences depending on the preparation approach:

-The NWs obtained in aqueous solution (W nanorods) display a compact morphology and a diameter ranged from 90 to 120 nm, caused by the non-uniformity of the nanochannels in the PC membrane (it can be observed in all the samples).

-W/IL microemulsions allows obtaining nanorods with a high density of well-defined non-spherical mesopores all over the entire area, even at the inner part of the wires, for both Pt and CoNi solutions (Figure 2c and d, respectively) forming a random network structure, as a consequence of the sintering of the electrodeposited metal inside the aqueous droplets in the microemulsion structure; the size of the mesopores was statistically measured to be approximately 2-5nm.

-Observation of the W+S nanorods for Pt and CoNi solutions (Figure 2e and f, respectively) reveals that this approach leads to mesoporous nanorods of platinum, with a high superficial porosity, with a pore size ranging from 6-9 nm. However, compact nanorods, apparently similar to those obtained in aqueous solution, were obtained in a CoNi classical bath. Therefore, it seems that the micelle system leads to good results (mesoporous nanorods) in diluted baths. However, when concentrated solution was used for the same amount of surfactant, the micelle system is distorted and it does not permit the formation of mesoporous structures.

-Finally, the use of polystyrene nanoparticles, with a diameter ranging from 10 to 50 nm (**Figure 2S**), dispersed in the aqueous solution (W+PS), has been demonstrated as a useful tool to obtain mesoporous nanorods with a random pore distribution and a non-uniform pore size distribution between 10 to 40 nm, according to the size distribution of the polystyrene NPs. However, in this case a double mesoporous nanostructure could be expected as a consequence of the presence of a surfactant as a suspension stabilizer.

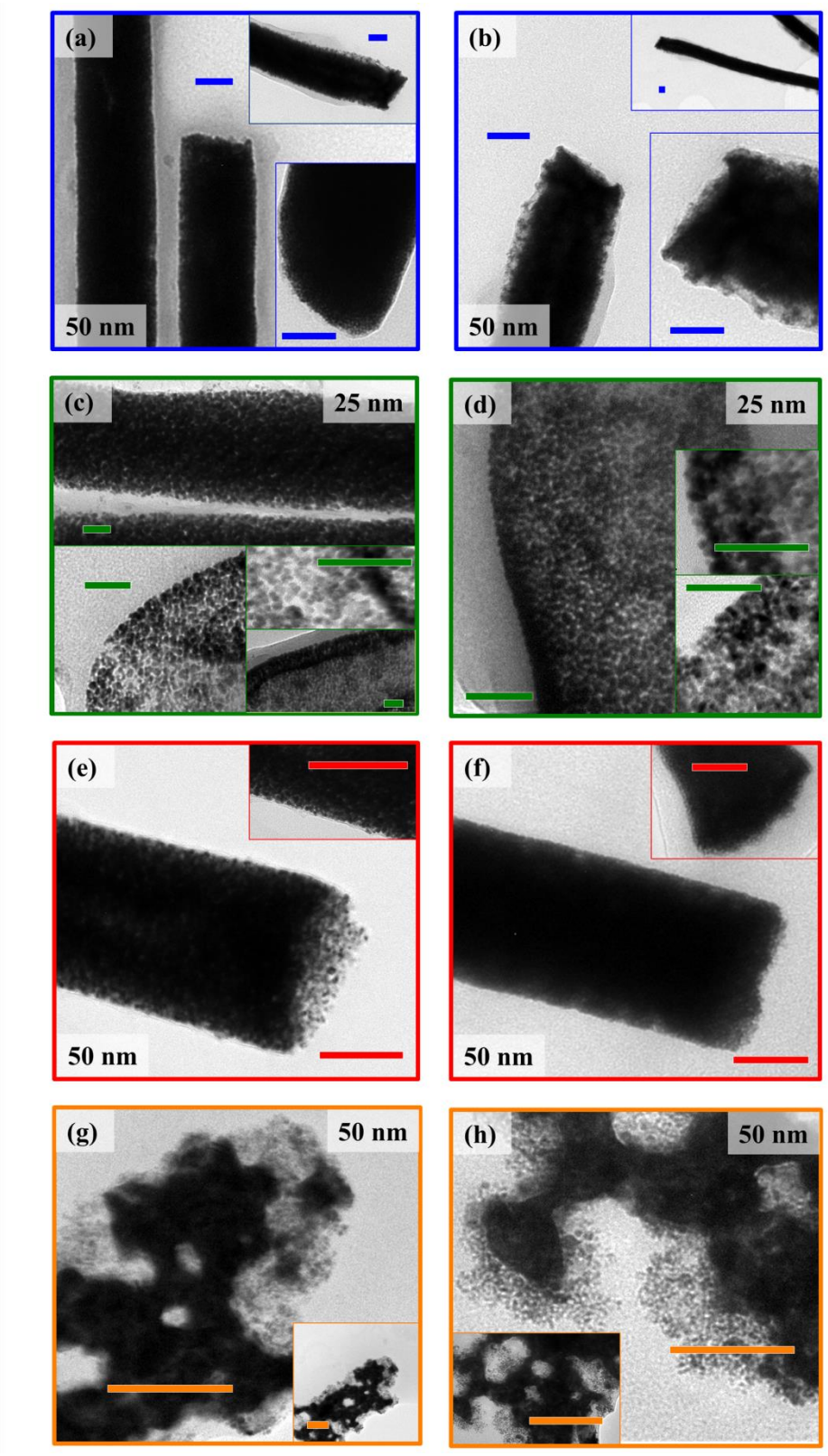

Figure 2: Transmission electron micrographs of Pt nanorods prepared in (a) aqueous solution (W), (c) water-in-ionic liquid microemulsion (W/IL), (e) surfactant solution (W+S) or (g) polystyrene suspension (W+PS) and CoNi@Pt nanorods prepared in (b) W, (d) W/IL, (f) (W+S) or (h) (W+PS).

The Electrochemically Active Surface Area (ECSA) of each electrocatalyst was measured by recording the hydrogen adsorption/desorption peaks in the cyclic voltammetries, in H_2SO_4 0.5M, of the different nanorods synthesized (**Figure 3**a and c, for Pt and CoNi@Pt nanorods, respectively). **Table 2** shows the calculated ECSA values of each electrocatalyst, which follow the tendency compact (W) < W+S < W+PS < W/IL for the Pt nanorods and compact (W) ~ W+S < W+PS < W/IT for the CoNi ones, as expected from the TEM images. The ECSA values for W nanorods of both Pt and CoNi@Pt, and W +S CoNi@Pt nanorods exhibit a similar surface area than other Pt nanorods reported in the literature, demonstrating their non-mesoporous structure. Moreover, W + PS nanorods of Pt and CoNi@Pt and W+ S nanorods of Pt exhibit around twice as much surface area as compact nanorods, as could be expected according to the measurements found in the literature for superficial mesoporous structures. Remarkably, both W/IL nanorods of Pt and CoNi@Pt exhibit much higher values than recent state-of-the-art Pt-based nanorods (around 10 times more than compact nanorods and 4 times more than other porous structures).[45, 48-51]These high ECSA values also reveal that the whole surface of the nanorods is electrochemically accessible, which is fundamental for electrocatalytic reactions.

We also investigated the durability of the electrocatalysts by determining the ECSA values after 200 cycles of treatment in H_2SO_4 0.5 M, between -0.28 and 1.2 V. It was found that the ECSA values of each electrocatalyst exhibited only a slight drop (smaller than 6 %) after the cycling treatment (Figure 3b and d, for Pt and CoNi@Pt nanorods, respectively), even in the core@shell structures. These results demonstrate that they have a significantly high stability. Furthermore, core@shell structures exhibit a similar behavior than pure Pt nanostructures.

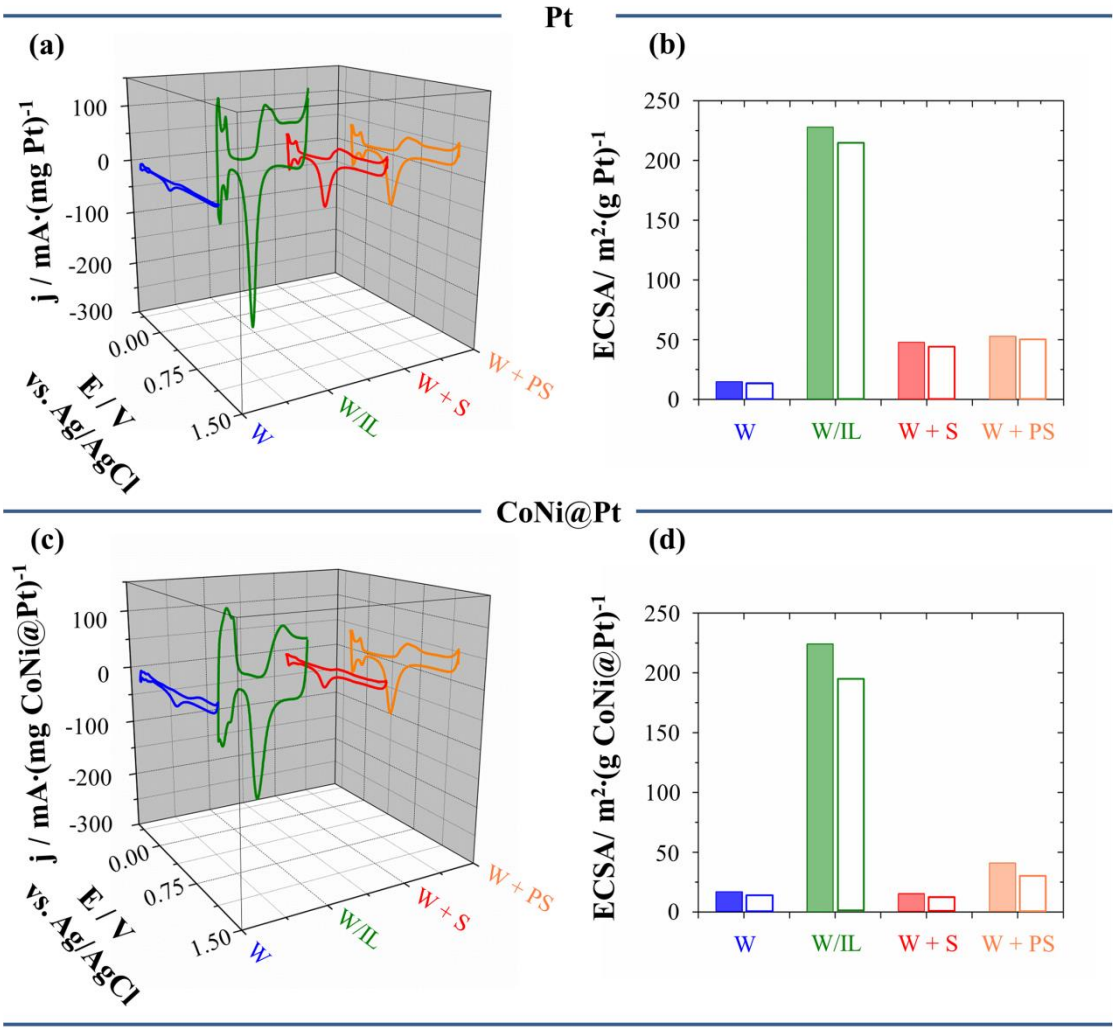

Figure 3: Cyclic voltammetry (first cycle) of different (a) Pt and (c) CoNi@Pt nanorods in H_2SO_4 0.5 M solutions at room temperature at the scan rate of 100 mV s^{-1}. ECSA values of different (b) Pt and (d) CoNi@Pt nanorods obtained in the first cycle (colored) and the 200th cycle (non-colored). The ECSAs are estimated assuming that the charge required to oxidize a mono-layer of hydrogen on bright Pt is 210 μC cm^{-2}.

Unfortunately, the highly acidic environment of an acidic fuel cell rapidly corrodes any surface accessible of non-noble metals, resulting in a leaching of the catalyst. CoNi nanorods should be protected from corrosion by the Pt shell. Therefore, the shell should guarantee the durability of our core@shell catalysts. For this reason, a complete shell of Pt is necessary. However, a too thick Pt shell could present properties no different than bulk Pt (non-synergetic effects) and obviously drive up the price of the catalyst. Therefore, in order to demonstrate the

stability and durability of the electrocatalyst, the corrosion tendency of the different nanorods synthesized were analyzed (**Figure 4**a and b, for Pt and CoNi@Pt, respectively). This stability test of the electrocatalysts was carried out after immersing the samples until attaining the steady-state potential (E_{ss}) in a solution of H_2SO_4 0.5 M. The log j vs. E curves of the different nanorods, obtained by a linear potentiodynamic sweep from E_{ss}-300 to +300 mV at 0.1 mV s^{-1}, show both the very positive corrosion potential in the aggressive sulfuric medium and the low slope of the anodic branch, which reveal the stability of the nanostructures and their low corrosion rate. Table 2 summarizes the corrosion potential of each nanowire in H_2SO_4 0.5 M, the non-dissolution of the CoNi@Pt in the sulfuric medium and the similar results in the accelerated corrosion test in the acidic environment respect to those of pure platinum corroborates, the complete shell of Pt of, the core@shell nanorods, even in their inner part, as could be expected according to the cycling treatment in acidic media described previously. The corrosion potential depends on the nanowire morphology and structure, resulting in the pure Pt nanorods being slightly more stable than the parallel CoNi@Pt structures. Although the corrosion potentials are very positive for the different nanorods, the mesoporous ones have the lower values, as could be expected taking into account their extraordinary surface area. Moreover, the Pt shell in W/IL nanorods should be thinner compared with that of W, W +S o W +PS nanorods because the amount of platinum in this catalyst represents only twice as much as the W nanorods, while the surface area is 15 times larger.

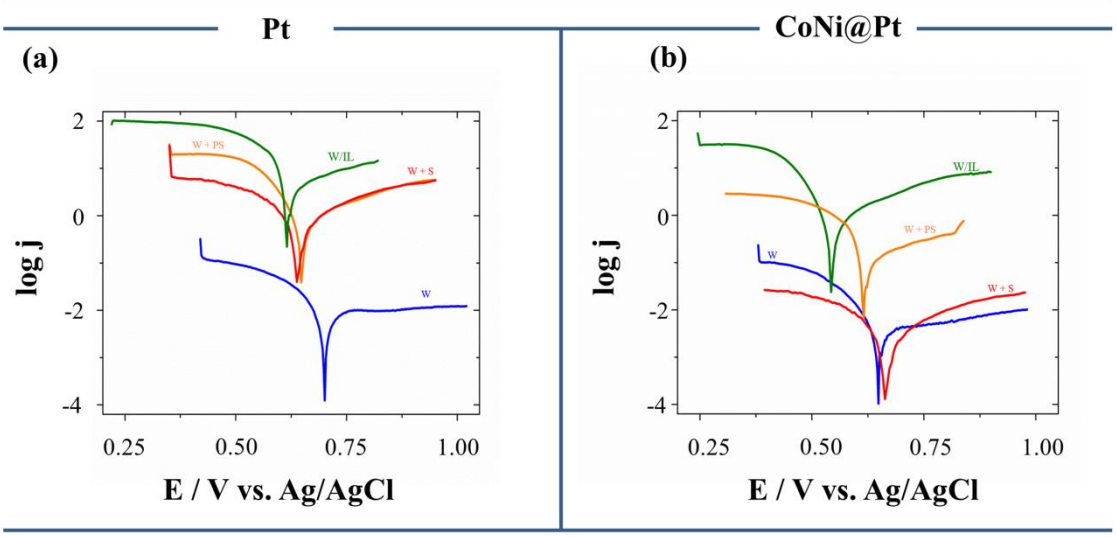

Figure 4: Potentiodynamic polarization curves in logarithmic scale corresponding to (a) Pt and (b) CoNi@Pt nanorods in H_2SO_4 0.5 M solutions.

The electrocatalytic performance toward the methanol oxidation of our eight types of nanorods was evaluated and compared. **Figure 5**a and c shows the electrocatalyst loading mass-normalized cyclic voltammograms of methanol oxidation obtained with different catalysts, in which the two characteristic methanol oxidation peaks are identified in the forward (which is ascribed to the freshly chemisorbed species) and backward (which is ascribed primarily to the removal of carbonaceous species that are not completely oxidized in the forward sweep) scans.

In the case of Pt, it is noticeable that the catalytic activity of the W/IL nanorods is significantly higher than that of the other catalysts, especially in comparison with the compact nanorods. As can be seen in Figure 5a W/IL, platinum nanorods show the highest mass-normalized current density (j_{max}) of 1285 mA mg^{-1}, as a consequence of a three-dimensionally interconnected network of platinum, rapidly accessible to the reactants, which is around 11.9, 3.2, and 3.0 times higher than that of W (108 mA mg^{-1}), W +S (399 mA mg^{-1}), and W + PS (430 mA mg^{-1}) nanorods. Also, for these extraordinarily porous W/IL nanorods, an important advance in the peak potential could be observed, which reveals the very good performance for the methanol oxidation. Moreover, we can compare the values of the forward anodic peak current density (j_f) and the reverse anodic peak current density (j_b) for each type of platinum

nanorods, because a low j_f/j_b ratio is used as an indicator of the CO-tolerance of electrocatalysts in MOR.[52] The j_f/j_b values were always greater than 1, specifically 1.20, 1.17, 1.19, and 1.52 for W, W/IL, W +S, and W +PS platinum nanorods, respectively. The higher ratio indicates more effective removal of poisonous carbonaceous species on the catalyst surface.

In the case of the CoNi@Pt core@shell structures, also the W/IL nanorods exhibit a significantly higher catalytic activity in comparison with the other core-shell catalysts. Moreover, all the CoNi@Pt nanorods, especially the W/IL ones, produce an important advance in the methanol oxidation peak respect to the parallel Pt nanorods of reference. Furthermore, the highest mass-normalized current density (j_{max}) of the CoNi@Pt W/IL nanorods (1326 mA mg^{-1}) is around 15.2, 12.2, and 4.4 times higher than the observed in W (87 mA mg^{-1}), W+S (109 mA mg^{-1}) and W+PS (301 mA mg^{-1}) nanorods, due to the total mesoporous network. Therefore, compact nanorods of both Pt and CoNi@Pt exhibit a similar mass-normalized current density than other nanorods described in the literature. Moreover, the superficial mesoporous structures (W+S nanorods of Pt) and the PS+W of both Pt and CoNi@Pt nanostructures show a higher mass-activity than commercial Pt/C (250 mA mg^{-1} in the same experimental conditions). Remarkably, the mass-normalized current densities of both Pt and CoNi@Pt W/IL nanorods were also higher than the state-of-the-art Pt-based nanorods, or other Pt nanomaterials reported previously (around 2 to 6 times more depending on the nanostructure, in the same experimental conditions.).[45, 53-55]

The j_f/j_b values were 2.89, 1.88, 2.81, and 3.26 for W, W/IL, W +S, and W +PS, respectively, values far higher than those corresponding to the pure Pt nanorods, which reveals that the CoNi@Pt nanorods present a higher good-poison tolerance. Hence the obtained W/IL mesoporous nanorods, especially the core@shell, could be proposed as a suitable electrocatalysts due to their extraordinary performance respect to the methanol oxidation. The values of the onset potential (E_{onset}), peak potential (E_p), maximum of the mass-normalized current density (j_{max}), mass-normalized current density at 0.6 V ($j_{0.6V}$) and the j_f/j_b ratio of all electrocatalysts are listed in Table 2. Accordingly, the peak potentials, the mass-normalized

current densities and the j_f/j_b values of core@shell structures show the synergetic effect of the CoNi core in the prepared electrocatalysts: the shell formation promotes an important shift in the peak potential, which enhances the catalytic performance, because it implies the presence of a thin layer of superficial Pt atoms, which interact electronically with the underlying base metal atoms (CoNi) by the contraction of the Pt-Pt bond distance or greater Pt 3d orbital vacancies.[56,57] Moreover, an important reduction of poisoning by adsorbed carbonaceous intermediates could be observed in the core@shell structures as a consequence of the interaction between de CoNi core and the Pt layer.[24-26]

Therefore, the mesoporous CoNi@Pt core@shell nanorods present the best performance for methanol oxidation in acidic medium because the present the highest amount of superficial Pt atoms and an improved active Pt, which make its promising electrocatalysts for the future.

Lastly, in order to analyze the long-term performance of the electrocatalysts toward the MOR under continuous operating conditions, chronoamperometric experiments were carried out. Figure 5b and c shows plots of mass-normalized current densities versus time recorded at 0.6 V for 3600 s for the different kind of Pt and CoNi@Pt nanorods. As can be seen in chronoamperometric curves, at short testing times, the oxidation current rapidly decays for all the electrocatalysts. However, after several minutes the current decay gradually slows down and remains pseudostable, demonstrating that the electrocatalytic stability under continuous operating conditions is higher in both W/IL nanorods of Pt and CoNi@Pt, compared with the other prepared catalysts.

TABLE 2. Catalyst Characterization and Catalytic Performance of different prepared nanorods.

System		Pt / at. %	ECSA / m^2 g^{-1}	E_{cor} / V	E_{onset} / V	j_{max} / mA · mg^{-1}	E_p / V	$j_{0.6V}$ / mA · mg^{-1}	j_f/j_b
W	Pt	100	15	0.70	-0.04	108	0.64	104	1.20
	CoNi@Pt	4	17	0.66	-0.01	87	0.51	64	2.89
W/IL	Pt	100	228	0.61	-0.18	1285	0.54	1022	1.17
	CoNi@Pt	8	224	0.55	-0.17	1326	0.50	1092	1.88
W+S	Pt	100	48	0.65	-0.06	399	0.63	381	1.19
	CoNi@Pt	3	15	0.67	-0.02	109	0.52	86	2.81
W+PS	Pt	100	53	0.64	-0.06	430	0.69	294	1.52

CoNi@Pt	6	41	0.62	-0.04	301	0.51	235	3.26

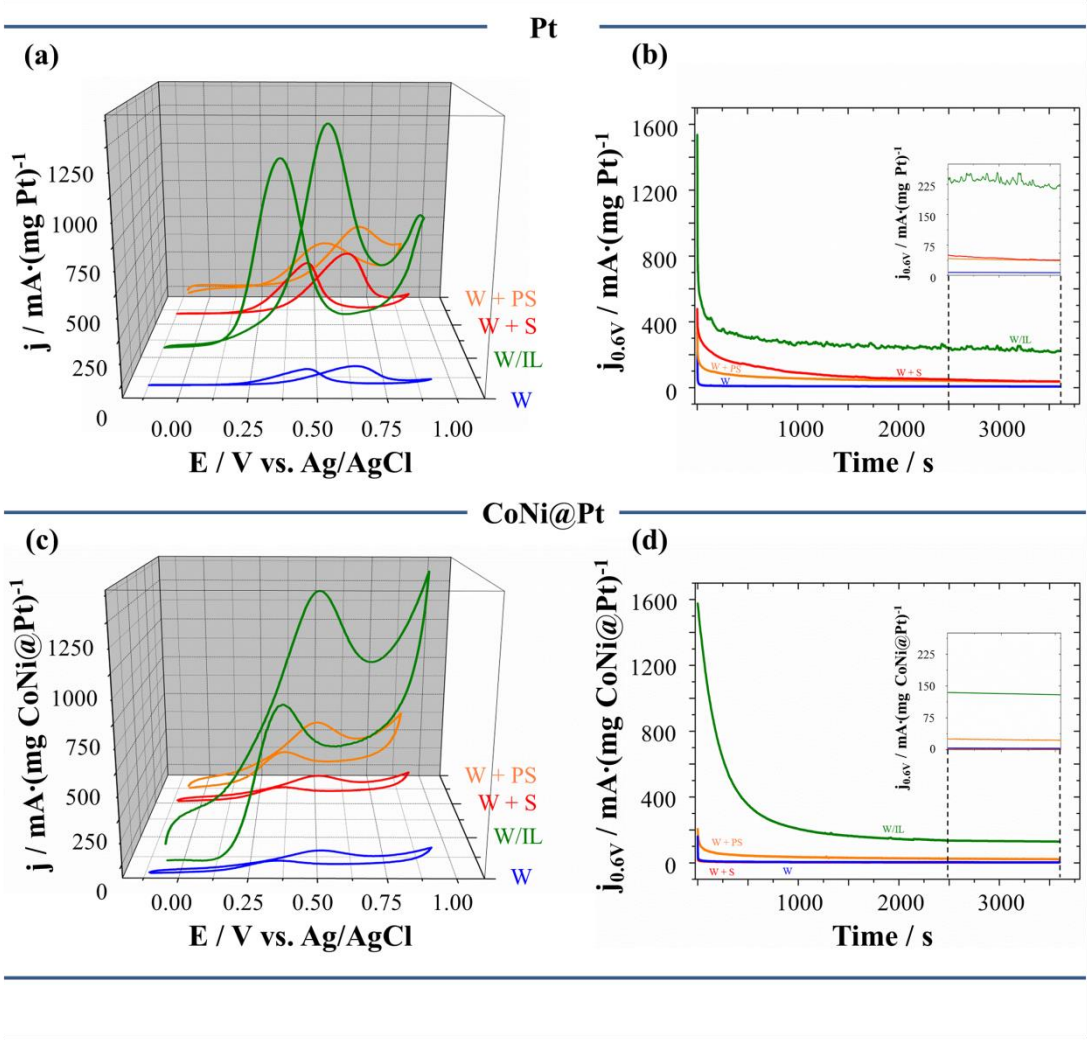

Figure 5: Cyclic voltammogramsat 50mV s^{-1} of (a) Pt and (b) CoNi@Pt nanorods, and chronoamperometric curves (recorded at 0.6V) of (b) Pt and (d) CoNi@Pt nanorods for methanol oxidation.

CONCLUSIONS

The electrochemical synthesis in different media (aqueous solution, water-in-ionic liquid microemulsion, micellar solution and suspension of polystyrene nanoparticles) of CoNi nanorods, followed by the formation of a shell of platinum, allowed us to obtain both compact and mesoporous CoNi@Pt nanorods. The micellar system, which is able to form mesoporous

pure platinum nanorods, does not permit the formation of mesoporous CoNi nanorods, probably due to the destruction of the micellar system in the presence of the concentrated solution of CoNi. The best performance as electrocatalyzers for methanol oxidation corresponds to the mesoporous core@shell nanorods obtained in suspension of polystyrene and, especially, in water-in-ionic liquid microemulsion. These nanorods present a very high active surface (224 m^2 g^{-1}), much more than that of compact nanorods, which demonstrated the porosity both in the surface and in the interior. Moreover, the presence of the CoNi core improves the performance of the platinum, inducing high activity in the superficial platinum of the shell and lower tendency to poisoning during the methanol oxidation. Therefore, a very high mass-normalized current density of 1326 mA mg^{-1}, a high j_f/j_b ratio and a clear advance of the methanol oxidation peak respect to pure platinum nanostructures turn the very mesoporous CoNi@Pt nanorods obtained in microemulsion with ionic liquids into a very promising electrocatalyzer for methanol oxidation in direct methanol fuel cells in acidic medium. The corrosion curves in sulfuric acid demonstrated the stability of the core@shell nanorods, which corroborates the good covering of the CoNi with platinum, and the maintenance of a significant current of methanol oxidation as a function of time reveals a good durability. The low percentage of the platinum shell in the mesoporous nanorods (8 at. %) implies a clear economic saving in the price of the electrocatalyzer. Finally, the magnetic character of the nanorods makes it easy to handle the nanostructures.

METHODS

Preparation of the Electrodeposition Media.

Four different systems have been used as electrodeposition media in order to obtain different types of nanorods. Herein, we report the composition and preparation procedure for each system.

- Pt and CoNi aqueous solution (W) contains 20 mM sodium hexacloroplatinate (IV) hexahydrate(Aldrich, 98 %) and 0.2 M Co (II) chloride (Carlo Erba, > 98.0 %) + 0.9 M Ni (II) chloride(Sigma Aldrich, > 98.0 %) + 30 gdm^{-3}boric acid (Merck, 99.8 %) + 4.5 mM saccharin (Merck) at a pH adjusted to pH = 4.5 with sodium hydroxide (Merck, >99 %) solutions, respectively. The both aqueous solutions were freshly prepared with double distilled water that was afterwards treated using a Millipore Q system with resistivity of 18.2 $M\Omega cm^{-1}$. These aqueous solutions were used to prepare a W/IL microemulsion and a micellar solution.
- The W/IL microemulsion was prepared by mixing aqueous solution (W), non-ionic surfactant (S), p-octyl polyethylene glycol phenyl ether a.k.a. Triton X-100 (Acros Organics, 98 %–), and ionic liquid (IL), 1-Butyl-3-methylimidazolium hexafluorophosphate a.k.a. bmimPF_6 (Acros Organics, 98 %–), in the selected proportions based on the literature (27.0 wt. % of W, 61.0 wt. % of S, and 12.0 wt. % of IL).[58,59]
- The Micellar solution (W +S) was prepared by stirring aqueous solution (W) and non-ionic surfactant (S), polyoxyethylene acyl ether*a.k.a.*Brij 58, in the selected proportions based on the literature (1.0 wt. % of S and 99.0 wt. % of W).[45]
- Polystyrene nanoparticle suspension (W + PS). The reagents in the same composition as in the aqueous solution for both Pt and CoNi solutions were dissolved in a polystyrene suspension of nanoparticles ranged from 10 to 50 nm. The polystyrene suspension was provided by Magsphere, Inc. This suspension was formed by 10.0 wt. % of polystyrene nanoparticles (PS), 88.0 wt. % of water, and 2.0 wt. % of non-ionic surfactant Sodium dodecyl sulfate (S).

Preparation of Nanorods.

Commercial polycarbonate (PC) membranes (Millipore Company) with a nominal pore size of 100 nm were used to synthesize Pt and CoNi nanorods using the previously described media. In order to use the polycarbonate filters as a working electrode a conductive layer on one side is

necessary. Therefore, vacuum evaporation was used to coat the membrane on one side with around a 100 nm-thick gold layer, enabling conductivity. Electrochemical fabrication of the nanorods was performed at room temperature (25^{o}C), with a microcomputer controlled by a potentiostat/galvanostat Autolab with PGSTAT30 equipment and GPES software, using a three-electrode electrochemical system with the described polycarbonate membranes, Pt spiral, and Ag/AgCl/ KCl (3M) as working, counter, and reference electrodes, respectively. The electrodeposition media were de-aerated before each experiment by argon bubbling. Remarkably, all the systems were maintained in semi-stirring conditions (Ar bubbling) during the process to promote the electrodeposition. After the deposition, the samples were immersed for 30 seconds into I_2/I^- saturated solution in order to dissolve the gold layer, and afterwards the polycarbonate membranes were dissolved with chloroform, and washed with chloroform (x10), ethanol (x5), and water (x5).

Nanorods Characterization.

Nanorods morphology was analyzed by a High-Resolution Transmission Electron Microscopy (Jeol 2100). An X-ray analyzer incorporated in a Leica Stereo Scan S-360 Equipment was used to determine the elemental composition.

Electrocatalytic Experiments.

Prior to the use of glassy carbon (GC) as a support, it was polished carefully with 0.3, and 0.5 µm of alumina powder and rinsed with milliQ water under sonication. Then, the support was allowed to dry under nitrogen. Then, a 5 µL of ink of nanorods prepared with water and 0.5 % Nafion® was dropped on the surface of the GC electrode and dried under nitrogen before the electrochemical experiments. All the electrochemical experiments were performed at room temperature using a three-electrode electrochemical cell with the prepared GC, a Pt spiral and Ag/AgCl/ KCl (3M)/ H_2SO_4 (0.5 M) as a working counter, and reference electrodes, respectively.

ASSOCIATED CONTENT

Supporting Information.

Chronoamperograms and Transmission Electron Images of polystyrene nanoparticles. This material is available free of charge via the Internet at http://pubs.acs.org.

AUTHOR INFORMATION

Corresponding Author

e.valles@ub.edu

Present Addresses

Departament de Química Física and Institut de Nanociència i Nanotecnologia (IN2UB), Universitat de Barcelona, Martí i Franquès 1, 08028, Barcelona, Spain.

ACKNOWLEDGMENT:

This work was supported by contracts CQT2010-20726 from MINECO. The authors wish to thank the *Centres Científics i Tecnològics de la Universitat de Barcelona* (CCiTUB) for allowing us to use their equipment. A.S. would also like to thank the *Ministerio de Educación, Cultura y Deporte* for its financial support (FPU grant).

REFERENCES:

(1) Dowland, S.; Lutz, T.; Ward, A.; King, S. P.; Sudlow, A.; Hill, M. S.; Molloy, K. C.; Haque, S. A. Direct Growth of Metal Sulfide Nanoparticle Networks in Solid-State Polymer Films for Hybrid Inorganic–Organic Solar Cells. *Adv. Mater.*,**2011**, 23, 2739–2744.

(2) Wang, W.-N.; An, W.-J.; Ramalingam, B.; Mukherjee, S.; Niedzwiedzki, D. M.; Gangopadhyay, S.; Biswas, P. Size and Structure Matter: Enhanced CO_2Photoreduction Efficiency by Size-Resolved Ultrafine Pt Nanoparticles on TiO_2 Single Crystals. J. *Am. Chem. Soc.*,**2012**, 134, 11276–11281.

(3) Pan, Y.;Shan, W.; Fang, H.; Guo,M.;Nie, Z.;Huang, Y.;Yao,S.Sensitive and Visible Detection of Apoptotic Cells on Annexin-V Modified Substrate Using AminophenylboronicAcid Modified Gold Nanoparticles (APBA-GNPs) Labeling.*Biosens. Bioelectron.*,**2013**,52C,62–68.

(4) Lei, Y.; Zhao, G.; Liu, M.; Zhang, Z.; Tong, X.; Cao, T. Fabrication, Characterization, and Photoelectrocatalytic Application of ZnO Nanorods Grafted on Vertically Aligned TiO_2 Nanotubes. *J. Phys. Chem. C*, **2009**, 113, 19067–19076.

(5) Kim, D. K.; Muralidharan, P.; Lee. H.-W.; Ruffo, R.; Yang, Y.; Chan, C. K., Peng, H.; Huggins, R. A.; Cu, Y. Spinel $LiMn_2O_4$ Nanorods as Lithium Ion Battery Cathodes. *Nano Lett.*, **2008**, 8, 3948–3952.

(6) Xui, S.; Sun, D.; Liu, H.; Wang, X.; Yan, X. Fabrication of Cu-doped cerium oxide nanofibers via electrospinning for preferential CO oxidation. *Catal. Commun.*,**2011**, 12, 514-518.

(7) Su, L.; Jia, W.; Schempf, A.; Ding, Y.; Lei, Y. Free-Standing Palladium/Polyamide 6 Nanofibers for Electrooxidation of Alcohols in Alkaline Medium. *J. Phys. Chem. C*, **2009**, 113, 16174–16180.

(8) Mundra, R. V.; Wu, X.; Sauer, J.; Dordick, J. S.; Kane, R. S. Nanotubes in Biological Applications. *Curr. Opin. Biotech.*,**2014**, 28, 25–32.

(9) Caicedo, H.; Dempere, L. A.; Vermerris, W. Template-mediated synthesis and bio-functionalization of flexible lignin-based nanotubes and nanowires. *Nanotechnology*, **2012**, 23, 105605–105617.

(10) Aricò, A.S.; Bruce, P.; Scrosati, B.; Tarascon, J.-M.; Van Schalkwijk, W. Nanostructured Materials for Advanced Energy Conversion and Storage Devices. *Nat. Mater.*,**2005**, 4, 366–377.

(11) Basri, S.; Kamarudin, S. K.; Daud, W. R. W.; Yaakub, Z. Int. Nanocatalysts for Direct Methanol Fuel Cell (DMFC). *Int.J. Hydrogen Energy*, **2010**, 35, 7957–7970.

(12) Candelaria, S. L.; Shao, Y.; Zhou, W.; Li, X.; Xiao, J.; Zhang, J.-G.; Wang, Y.; Liu, J.; Li, J.; Cao, G. Nanostructured Carbon for Energy Storage and Conversion. *Nano Energy*, **2012**, 1, 195–220.

(13) Li, Q.; He, R.; Jensen, J. O.; Bjerrum, N. J. Approaches and Recent Development of Polymer Electrolyte Membranes for Fuel Cells Operating above 100 °C. *Chem. Mater.*, **2003**, 15, 4896–4915.

(14) Neburchilov, V.; Martin, J.; Wang, H.; Zhang, J. A review of Polymer Electrolyte Membranes for Direct Methanol Fuel Cells. *J. PowerSources*, **2006**,169, 221– 238.

(15) Kamarudin, S. K.; Daud, W.R.W.; Ho, S. L.; Hasran, U. A. Overview on the Challenges and Developments of Micro-Direct Methanol Fuel Cells (DMFC). *J. Power Sources*,**2006**,163, 743– 754.

(16) Antolini, E. Formation of Carbon-Supported PtM Alloys for Low Temperature Fuel Cells: a Review. *Mater. Chem. Phys.* **2003**, 78, 563– 573.

(17) Guo, S.; Dong, S.; Wang, E. Three-Dimensional Pt-on-Pd Bimetallic Nanodendrites Supported on Graphene Nanosheet: Facile Synthesis and Used as an Advanced Nanoelectrocatalyst for Methanol Oxidation. *ACS Nano*, **2010**, 4, 547– 555.

(18) Liu, Z.; Shi, Q.; Zhang, R.; Wang, Q.; Kang, G.; Peng, F. Phosphorus-Doped Carbon Nanotubes Supported Low Pt Loading Catalyst for the Oxygen Reduction Reaction in Acidic Fuel Cells. *J. Power Sources*,**2014**,268, 171– 175.

(19) Zheng, J.-S.; Tian, T.; Gao, Y.; Wu, Q.; Ma, J.-X.; Zheng, J.-P. Ultra-Low Pt Loading Catalytic Layer Nased on Buckypaper for Oxygen Reduction Reaction.*Int.J. Hydrogen Energy*, **2014**, 39, 13816–13823.

(20) Maier, W. D.; Marsh, J. S.; Barnes, S.-J, Dodd, D. C. The Distribution of Platinum Group Elements in the Insizwa Lobe, Mount Ayliff Complex, South Africa: Implications for Ni-Cu-PGE Sulfide Exploration in the Karoo Igneous Province. *Econ. Geol.*,**2002**, 97, 1239-1306.

(21) Wang, H.; Wang, L.; Sato, T.; Sakamoto, Y.; Tominaka, S.; Miyasaka, K.; Miyamoto, N.; Nemoto, Y.; Terasaki, O.; Yamauchi, Y. Synthesis of Mesoporous Pt Films with

Tunable Pore Sizes from Aqueous Surfactant Solutions. *Chem. Mater.*,**2012**, 24, 1591–1598.

(22) Wu, J. B.; Li, Z. G.; Huang, X. H.; Lin, Y. Porous Co_3O_4/NiO Core/Shell Nanowire Array with Enhanced Catalytic Activity for Methanol Electro-Oxidation. *J. Power Sources*,**2013**,224, 1– 5.

(23) Yang, H.; Wang, H.; Ji, S.; Linkov, V.; Wang, R. Synergy between Isolated-Fe_3O_4 Nanoparticles and CN_x Layers Derived from Lysine to Improve the Catalytic Activity for Oxygen Reduction Reaction. *Int.J. Hydrogen Energy*, **2014**, 39, 3739–3745.

(24) Mu, R.; Fu, Q.; Xu, H.; Zhang, H.; Huang, Y.; Jiang, Z.; Zhang, S.; Tan, D.; Bao, X. Synergetic Effect of Surface and Subsurface Ni Species at Pt−Ni Bimetallic Catalysts for CO Oxidation. *J. Am. Chem. Soc.*, **2011**, 133, 1978–1986.

(25) Antolini, E.; Salgado, J. R. C.; Gonzalez, E. R. The Stability of Pt–M (M = first row transition metal) Alloy Catalysts and Its Effect on the Activity in Low Temperature Fuel Cells: a Literature Review and Tests on a Pt–Co Catalyst. *J. Power Sources*,**2006**,160, 957– 968.

(26) Antolini, E.; Salgado, J. R. C.; Gonzalez, E. R. The Methanol Oxidation Reaction on Platinum Alloys with the First Row Transition Metals: the Case of Pt–Co and– Ni Alloy Electrocatalysts for DMFCs: a Short Review. *Appl. Catal.* B, **2006**, 63, 137-149.

(27) Ding, L.-X.; Li, G.-R.; Wang, Z.-L.; Liu, Z.-Q.; Liu, H.; Tong,Y.-X. Porous Ni@Pt Core-Shell Nanotube Array Electrocatalyst with High Activity and Stability for Methanol Oxidation. *Chem. Eur. J.***2012**, 18, 8386-8391.

(28) Cao, M.; Wu, D.; Cao, R. Recent Advances in the Stabilization of Platinum Electrocatalysts for Fuel-Cell Reactions. *ChemCatChem*, **2014**, 6, 26-45.

(29) Vega, A. A.; Newman, R.C. Nanoporous Metals Fabricated through Electrochemical Dealloying of Ag-Au-Pt with Systematic Variation of Au:Pt Ratio. *J. Electrochemical. Soc.* **2014**, 161, C1-C10.

(30) Wu, Y.; Cheng, G.; Katsov, *K.;* Sides, *S. W.;* Wang, *J.;* Tang, *J.;* Fredrickson, *G. H.;* Moskovits, *M.;* Stucky,*G.D.* Composite Mesostructures by Nano-Confinement. *Nat. Mater.*,**2004**, 3, 816–822.

(31) Wang, H.; Jeong, H. Y.; Imura, M.; Wang, L.; Radhakrishnan, L.; Fujita, N.; Castle, T.; Terasaki, O.; Yamauchi, Y. Shape- and Size-Controlled Synthesis in Hard Templates: Sophisticated Chemical Reduction for Mesoporous Monocrystalline Platinum Nanoparticles. *J. Am. Chem. Soc.*,**2011**, 133, 14526–14529.

(32) Shim, J.; Lee, J.; Ye, Y.; Hwang, J.; Kim, s.-K.; Lim, T.-H.; Wiesner, U.; Lee, J. One-Pot Synthesis of Intermetallic Electrocatalysts in Ordered, Large-Pore Mesoporous Carbon/Silica toward Formic Acid Oxidation. *ACS Nano*, **2012**, 6, 6870-6881.

(33) Sievers, G.; Mueller, S.; Quade, A.; Steffen, F.; Jakubith, S.; Kruth, A.; Brueser, V. Mesoporous Pt–Co oxygen reduction reaction (ORR) catalysts for low temperature proton exchange membrane fuel cell synthesized by alternating sputtering. *J. Power Sources,***2014**,268, 255– 260.

(34) Zhu, C.; Guo, S.; Dong, S. Rapid, General Synthesis of PdPt Bimetallic Alloy Nanosponges and Their Enhanced Catalytic Performance for Ethanol/Methanol Electrooxidation in an Alkaline Medium. *Chem. Eur. J.*,**2013**, 19, 1104-1111.

(35) Jin, J.; Fu, X.; Liu, Q.; Zhang, J. A Highly Active and Stable Electrocatalyst for the Oxygen Reduction Reaction based on a Graphene-Supported g-C_3N_4@cobalt Oxide Core–Shell Hybrid in Alkaline Solution. ***J***. *Mater. Chem. A***, 2013,**1, 10538-10545.

(36) Sánchez-Padilla, N. M.; Morales-Acosta, D.; Morales-Acosta, M. D.; Montemayor, S. M.; Rodríguez-Varela, F. J.Catalytic Activity and Selectivity for the ORR of Rapidly Synthesized M@Pt (M = Pd, Fe_3O_4, Ru) Core–Shell Nanostructures. *Int. J. Hydrogen Energy*, ***2014****, 39, 16706-1671.*

(37) Xiao, J.; Wan, L.; Wang, X.; Kuang, Q.; Dong, S.; Xiao, F.; Wang, S. Mesoporous Mn_3O_4–CoOCore–Shell Spheres Wrapped by Carbon Nanotubes: a High Performance Catalyst for the OygenReduction Reaction and CO Oxidation. *J. Mater. Chem. A*, **2014**,2, 3794-3800.

(38) Wang, H.; Xu, C.; Cheng, F.; Zhang, M.; Wang, S.; Jiang, S. P. Pd/Pt Core–Shell Nanowire Arrays as Highly Effective Electrocatalysts for Methanol Electrooxidation in Direct Methanol Fuel Cells. *Electrochem. Commun.*,**2008**, 10, 1575-1578.

(39) Tong, Y.; Pu, J.; Wang, H.; Wang, S.; Liu, C.; Wang, Z. Ag–Pt Core–Shell Nanocomposites for Enhanced Methanol Oxidation. *J. Electroanal. Chem.* **2014**, 728, 66-71.

(40) Wu, Z.; Li, Q.; Feng, D.; Webley, P. A.; Zhao, D. Ordered Mesoporous Crystalline γ-Al_2O_3 with Variable Architecture and Porosity from a Single Hard Template. *J. Am. Chem. Soc.*, **2010**, 132, 12042–12050.

(41) Joo, S. H.; Choi, S. J.; Oh, I.; Kwak, J.; Liu, Z:; Terasaki, O.; Ryoo, R. Ordered Nanoporous Arrays of Carbon supporting High Dispersions of Platinum Nanoparticles. *Nature*, **2001**, 412, 169-172.

(42) Attard, G. S.; Leclerc, S. A. A.; Maniguet, S.; Russell, A. E.; Nandhakumar, I.; Bartlett, P. N. Mesoporous Pt/Ru Alloy from the Hexagonal Lyotropic Liquid Crystalline Phase of a Nonionic Surfactant. *Chem. Mater.*, **2001**, 13, 1444–1446.

(43) Zhang, X.; Lu, W.; Dai, J.; Bourgeois, L.; Hao, N.; Wang, H.; Zhao, D.; Webley, P.A. Ordered Hierarchical Porous Platinum Membranes with Tailored Mesostructures. *Angew. Chem. Int. Ed. Engl.* **2010**, 122, 10299-10303.

(44) Serrà, A.; Montiel, M.; Gómez, E.; Vallés, E. Electrochemical Synthesis of Mesoporous CoPt Nanowires for Methanol Oxidation. *Nanomaterials*, **2014**, 4, 189-202.

(45) Li, C.; Sato, T.; Yamauchi, Y. Electrochemical Synthesis of One-Dimensional Mesoporous Pt Nanorods Using the Assembly of Surfactant Micelles in Confined Space. *Angew. Chem. Int. Ed. Engl.* **2013**, 125, 8208-8211.

(46) Vilana, J.; Gómez. E.; Vallés, E. Electrochemical Control of Composition and Crystalline Structure of CoNi Nanowires and Films Prepared Potentiostatically from a Single Bath. *J. Electroanal. Chem.* **2013**, 703, 88-96.

(47) Vega, V.; Böhnert, T.; Martens, S.; Waleczek, M.; Montero-Moreno, J. M.; Görlitz, D.; Prida, V. M.; Nielsch, K. Tuning the Magnetic Anisotropy of Co–Ni Nanowires:

Comparison between Single Nanowires and Nanowire Arrays in Hard-Anodic Aluminum Oxide Membranes. *Nanotechnology*, **2012**, 23, 465709-465719.

(48) Ho, V. T. T.; Nguyen, N- G.; Pan, C.-J.; Cheng, J.-H.; Rick, J.; Su, W.-N.; Lee, J.-F.; Sheu, H.-J. Advanced Nanoelectrocatalyst for Methanol Oxidation and Oxygen Reduction Reaction, Fabricated as One-Dimensional Pt Nanowires on Nanostructured Robust $Ti_{0.7}Ru_{0.3}O_2$ Support. *Nano Energy*, **2012,** 1, 687-695.

(49) Choi, S. M.; Kim, J. H.; Jung, J. Y.; Yoon, E. Y.; Kim, W. B.Pt Nanowires Prepared via a Polymer Template Method: Its Promise Toward High Pt-Loaded Electrocatalysts for Methanol Oxidation. *Electrochim. Acta*, **2008**, 53, 5804-5811.

(50) Li, B.; Higgins, D. C.; Xiao, Q.; Yang. D.; Zhng, C.; Cai, M.; Chen, Z.; Ma, J. The Durability of Carbon Supported Pt Nanowire as Novel Cathode Catalyst for a 1.5 kW PEMFC Stack. *Appl. Catal. B Environ.*,**2015**, 162, 133-140.

(51) Huang, Z.; Zhou, H.; Chen,Z.; Zeng, F.; Chen, L.; Luo, W.; Kuang, Y. Facile Synthesis of Porous Pt Botryoidal Nanowires and their Electrochemical Properties. *Electrochim. Acta*, **2014,** 147, 643-649.

(52) Yuan, Q.; Duan, D.; Ma, Y.; Wei, G.; Zhang, Z.; Hao, X.; Liu, S. Performance of Nano-Nickel Core Wrapped with Pt Crystalline Thin Film for Methanol Electro-Oxidation. *J. Power Sources*,**2014**,245, 886– 891.

(53) Liu, L.; Pippel, E.; Scholz, R.; Gösele, U. Nanoporous Pt−Co Alloy Nanowires: Fabrication, Characterization, and Electrocatalytic Properties. *Nano Lett.*,**2009**, 9, 4352-4358.

(54) Chen, X.; Si, C.; Gao, Y.; Frenzel, J.; Sun, J.; Eggeler, G.; Zhang, Z. Multi-Component Nanoporous Platinum–Ruthenium–Copper–Osmium–Iridium Alloy With Enhanced Electrocatalytic Activity Towards Methanol Oxidation and Oxygen Reduction. *J. Power Sources*,**2015**,1, 324– 332.

(55) Liao, H.; Zhu, J.; Hou, Y. Synthesis and Electrocatalytic Properties of PtBiNanoplatelets and PdBi Nanowires.*Nanoscale*,**2014**, 6, 1049-1055.

(56) Alayoglu, S.; Nilekar, A. U.; Mavrikakis, M.; Eichhorn,B. Ru-Pt Core-Shell Nanoparticles for Preferential Oxidation of Carbon Monoxide in Hydrogen. *Nat. Mater.*, **2008,** 7, 333-338.

(57) Stamenkovic, V. R.; Fowler, B.; Mun, B. S.; Wang, G.; Ross, P. N.; Lucas, C. A.; Marcović, N. M. Improved Oxygen Reduction Activity on $Pt_3Ni(111)$ Via Increased Surface Site Availability. Science, **2007**, 315, 493-497.

(58) Serrà, A.; Gómez, E.; López-barbera, J. F.; Nogués, J.; Vallés, E. Green Electrochemical Template synthesis of CoPt Nanoparticles with Tunable Size, Composition, and Magnetism from Microemulsions Using an Ionic Liquid ($bmimPF_6$). *ACS Nano*, **2014**, 8, 4630-4639.

(59) Gao, Y.; Han, S.; Han, B.; Li, G.; Shen, D.; Li, Z.; Du, J.; Hou, W.; Zhang, G. TX-100/Water/1-Butyl-3-methylimidazolium Hexafluorophosphate Microemulsions. *Langmuir*, **2005**, 21, 5681-5684.